http://dx.doi.org/10.5012/bkcs.2013.34.12.3909

# Simple Crystal Phase Control of $TiO_2$ Nanoparticles *via* Pulsed Laser Ablation in Nitric Acid

**Seong Min Hong, Seulki Lee, Hyeon Jin Jung, Yiseul Yu, and Myong Yong Choi***

*Department of Chemistry and Research Institute of Natural Science, Gyeongsang National University, Jinju 660-701, Korea*
**E-mail: mychoi@gnu.ac.kr*
*Received September 6, 2013, Accepted September 25, 2013*

**Key Words :** $TiO_2$ nanoparticles, Anatase, Rutile, Pulsed laser ablation in liquid (PLAL)

It has long been known that anatase, brookite, and rutile are the major crystalline structures of $TiO_2$, of which the rutile phase is the most stable; whereas anatase and brookite phases are metastable and easily transformed to the rutile phase by heating above about 600-800 °C.[1] A number of investigations have been made on controlling the crystal structure and morphology of $TiO_2$ using a variety of synthetic methods, such as by hydrolysis of $Ti^{4+}$ ions,[2] hydrolysis of titanium alkoxides[3] or titanium tetrachloride[4] in the gas phase, sol-gel,[5] hydrothermal hydrolysis,[6] and precipitation.[7] Furthermore, a variety of attempts have been made to enhance the photocatalytic effects of $TiO_2$, including metallic and non-metallic doping, nano-size reduction, and its use in bi-metallic catalysis.[8] However, there is no report on the selective synthesis of the different phases of $TiO_2$ nanoparticles, involving different ratios of anatase and rutile, prepared in an ambient environment, *i.e.*, through the variation of $HNO_3$ concentration, without extreme temperature and pressure conditions.

Here, we present an approach that differs from the previously mentioned methods for the synthesis of $TiO_2$ nanoparticles. In our case we have employed a pulsed laser to ablate a Ti plate immersed in water. Pulsed laser ablation in liquid (PLAL)[9] has been demonstrated to be a simple, versatile, and clean method for preparing metal and metal oxide nanomaterials due to the use of high purity starting materials, no requirement for a catalyst, and reduced by-products, provided an appropriate metal and liquid is chosen.[10] Recent studies have demonstrated that PLAL of metal plates employing different parameters, such as laser wavelength, power, and the presence of surfactants, can lead to different products, sizes, and/or morphologies. Nonetheless, there are few reports of the formation of $TiO_2$ *via* PLAL. Furthermore, most studies have focused on the preparation of anatase and rutile $TiO_2$ in the absence/presence of surfactants; however, the systematic preparation employing different ratios of anatase/rutile $TiO_2$ has not been studied before. In this work, we have controlled the ratios of anatase/rutile $TiO_2$ nanoparticles by changing the concentration of $HNO_3$.

XRD measurements of the samples were employed in order to determine the crystal structure and the crystallinity of the prepared $TiO_2$ samples prepared *via* PLAL. The XRD patterns illustrated in Figure 1 correspond to the crystalline phases of the $TiO_2$ samples prepared *via* PLAL using various concentrated $HNO_3$ solutions. Figure 1(a), (b), and (c) present XRD patterns over a scan interval from 10 to 90° for the as-is sample of $TiO_2$ *via* PLA in DI water (a), $10^{-3}$ M (b), and 1 M solution of $HNO_3$ (c), respectively. It is seen that the XRD patterns for samples, (a) and (c), obtained *via* PLA in DI water and 1 M $HNO_3$ solution match the standard anatase (JCPDS number: 00-021-1272) and rutile (JCPDS number: 00-021-1276) patterns, respectively. The XRD pattern shown in Figure 1 (b) indicates that mixed phases of $TiO_2$, anatase and rutile are formed in $10^{-3}$ M $HNO_3$ solution. While it is generally the case that rutile $TiO_2$ is fabricated from calcination of anatase $TiO_2$ above 600-800 °C; in this work the rutile phase is simply and selectively obtained in 1 M $HNO_3$ solution at ambient conditions. According to the XRD patterns shown in (a), (b), and (c), the peaks are broader than those in (d), (e), and (f). From the Scherrer equation, peak broadness is inversely related to the full width at half maximum of an individual peak; the broader peak, the smaller crystallite size. Thus, it is apparent that the $TiO_2$ nanoparticles prepared at low concentrations of $HNO_3$ (Figure 1(a)-(c)) were smaller than the particles produced at higher

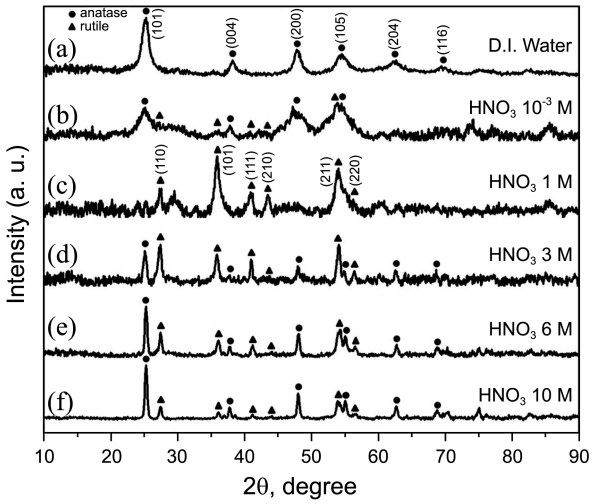


**Figure 1.** XRD patterns of the $TiO_2$ nanocrystals prepared *via* PLA on the Ti plate in (a) DI water, (b) $10^{-3}$, (c) 1, (d) 3, (e) 6, (f) 10 M $HNO_3$ solution [●: anatase, ▲: rutile].

concentrations of $HNO_3$ (Figure 1(d)-(f)) (see later).

Furthermore, it was observed that the ratio of anatase to rutile phase was increased gradually with increase in the $HNO_3$ concentration in the PLAL process. Increasing the concentration of $HNO_3$ not only gives rise to an increase of anatase ratio with respect to rutile, but also to the sharpness of the XRD peaks, as shown in Figure 1(d)-(f) compared to that for (b). This indicates that mixed phases of $TiO_2$ nanoparticles with different ratios were formed, and that both the crystallinity and the size of the particles were increased as the concentration of $HNO_3$ was increased. Previously, pure anatase $TiO_2$ nanoparticles were produced *via* PLA in DI water[11]; while, pure rutile $TiO_2$ was synthesized *via* PLA in poly(vinylpyrrolidone) solution.[12] However, in this work, pure anatase, rutile and a mixture of both phases have been selectively synthesized *via* PLAL using simple concentration control of $HNO_3$ solution.

In order to investigate the effect of the acid on the formation of $TiO_2$ nanoparticles, we employed concentrated HCl as the acidic solvent, instead of $HNO_3$. However, no significant formation of $TiO_2$ nanoparticles was identified in this case. Thus, the main factor for the production of $TiO_2$ nanoparticles *via* PLAL is the presence of an oxygen atom source in the acid solvent.[13] However, unfortunately, the detailed understanding of the formation of different phases of $TiO_2$ nanoparticles is beyond the scope of the present study.

Figure 2(a)-(f) presents the SEM images of $TiO_2$ nanoparticles obtained *via* PLAL employing various concentrations of $HNO_3$: 0, $10^{-3}$, 1, 3, 6, and 10 M, respectively. From the micrographs, the particles are nearly spherical. However, filamentous species were formed when the concentration of $HNO_3$ reached 10 M.

Filamentous species had also been observed previously when the initial PLA species were left in the dark for several weeks.[14] They may be formed through the agglomeration of $TiO_2$ clusters formed at the higher concentrations of $HNO_3$. Furthermore, it is also noted that the average size of $TiO_2$ nanoparticles (a) and (b) is smaller than that of the remainder. At a high $HNO_3$ concentration, larger sized-nanoparticles and filamentous species occur as seen in Figure 2(f).

TEM micrographs were obtained to investigate the size and shape of the $TiO_2$ nanocrystals prepared in DI water and

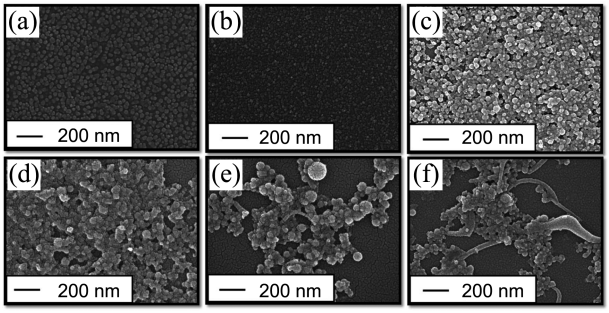


**Figure 2.** FE-SEM images of the $TiO_2$ nanoparticles prepared *via* PLA in (a) DI water, (b) $10^{-3}$, (c) 1, (d) 3, (e) 6, (f) 10 M $HNO_3$ solution.

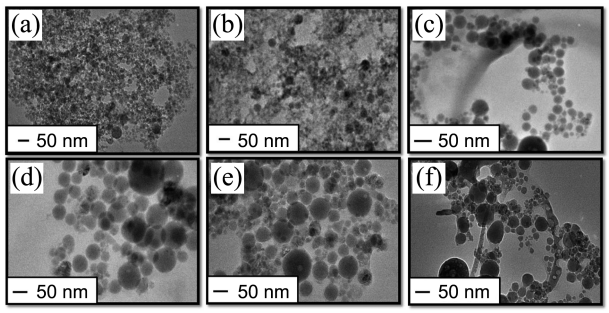


**Figure 3.** TEM images of the $TiO_2$ nanoparticles prepared *via* PLA in (a) DI water, (b) $10^{-3}$, (c) 1, (d) 3, (e) 6, (f) 10 M $HNO_3$ solution.

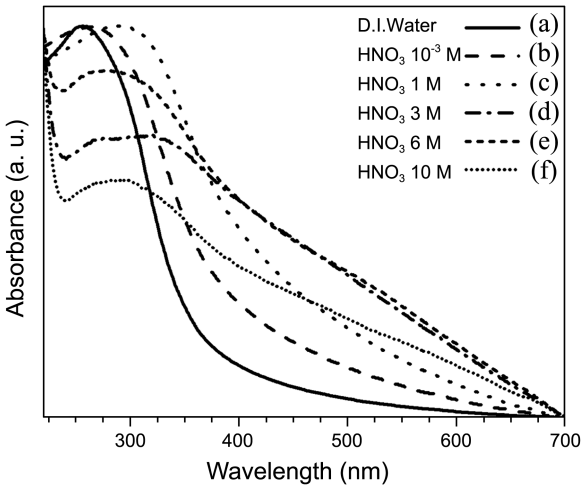


**Figure 4.** UV-Vis absorption spectra of $TiO_2$ prepared *via* PLA in (a) DI water, (b) $10^{-3}$, (c) 1, (d) 3, (e) 6, (f) 10 M $HNO_3$ solution.

at various concentrations of $HNO_3$ (Figure 3). Similar to the SEM images, the TEM images given in Figure 3(a) and (b), taken from laser ablation onto the Ti metal in DI water and $10^{-3}$ M $HNO_3$ respectively, found to be exhibited small spherical shaped nanoparticles. However, the spherical nanoparticles were larger when the concentration of the $HNO_3$ solution increased, as shown in Figure 3(c)-(f). Furthermore, filamentous species were also observed in the image corresponding to 10 M $HNO_3$.

The UV-Vis spectra of the solutions containing $TiO_2$ nanoparticles in the respective $HNO_3$ solutions are shown in Figure 4. The distinctive absorption bands lower than 390 nm can be attributed to absorption caused by the excitation of electrons from the valence to conduction band of $TiO_2$. Exciton absorption band maximum located at about 265 nm is very distinctive for the anatase $TiO_2$ band gap, which is both well-known and widely reported.[15] Since the $TiO_2$ nanoparticles prepared in higher than 1 M $HNO_3$ solution are a mixture of both anatase and rutile phases, the absorption spectra shown in Figure 4(c)-(f) exhibit a distinctive two band structure, where the higher and lower energy bands are attributed to the anatase and rutile phases, respectively. In agreement with this, the $TiO_2$ nanoparticles prepared *via* PLA in DI water and 1 M $HNO_3$ solution are seen to corre-

spond to anatase and rutile phases, respectively.

In summary, we have selectively synthesized anatase, rutile, and a mixture of these phases as $TiO_2$ nanoparticles *via* employing pulsed laser ablation in $HNO_3$ solutions of various concentrations. In the absence of $HNO_3$ (*i.e.* in DI water), only pure anatase $TiO_2$ nanoparticles were formed; however, in 1 M $HNO_3$ solution, only pure rutile $TiO_2$ nanoparticles were obtained. At a midway between these two concentrations, namely for $10^{-3}$ M $HNO_3$, a mixture of the both phases was generated. Further increase of the $HNO_3$ concentration gives rise to the enhancement of anatase compared to the rutile phase, which enables to the control of the ratio of anatase/rutile $TiO_2$. We speculate that the $TiO_2$ crystal phases are influenced by the amount of oxygen atom sources in the solvent used in PLAL, but this hypothesis remains to be tested. This procedure can be employed to selectively synthesize individual and mixed $TiO_2$ phases and control the size of the mixed phase nanoparticles by simply varying the concentration of $HNO_3$ under ambient experimental conditions. We propose that this simple method for producing selectively different anatase or rutile phases $TiO_2$ nanoparticles as well as for the control of the anatase/rutile ratio provides a very promising tool for the design and synthesis of highly active $TiO_2$ photocatalysts.

## Experimental

The experimental setup for the generation of metal nanoparticles *via* PLAL is described in detail elsewhere.[10] Briefly, the Ti (99.999%, Sigma-Aldrich) plate was fixed in a Pyrex vial filled with de-ionized (DI) water (10 mL) and the $HNO_3$ solution under a nitrogen purge continuously stirred by a magnetic bar. A pulsed Nd:YAG laser (1064 nm, 10 Hz, 7 ns) was focused onto the surface of the Ti plate with a spot size of about 1 mm diameter using a lens with a focal length of 25 mm. Laser ablation was continued for 30 min with a laser pulse energy of 80 mJ/pulse. The $HNO_3$ solutions used for PLAL were prepared at concentrations of $10^{-3}$, 1, 3, 6, and 10 M. The ablated solutions were washed several times with DI water using a centrifugation rate of 13000 rpm for 10 min to remove $HNO_3$. The resulting sediments were collected and then individually sonicated after addition of DI water and centrifugation. This washing procedure was repeated several times. Each experiment was repeated at least 10 times and the sediments were collected and dried on a silicon substrate at room temperature. The morphology and structure of the nanoparticles produced by PLAL were investigated with a field emission scanning electron microscope [FE-SEM, XL30 S FEG, Philips (15 kV)] and transmission electron microscope [TEM, JEOL, JEM-2-10 (200 kV)]. X-ray diffraction (XRD) patterns of the nanoparticles were obtained with a Bruker AXS D8 DISCOVER with GADDS diffractometer using Cu Kα (0.1542 nm) radiation with a Bragg angle ranging from 10 to 90°.

**Acknowledgments.** This work was supported by the Korea Ministry of Environment as "GAIA Project" (2012000550026).

## References

1. Chen, X.; Mao, S. S. *Chem. Rev.* **2007**, *107*, 2891.
2. Matijeviæ, E.; Budnik, M.; Meites, L. *J. Colloid Interface Sci.* **1977**, *61*, 302.
3. Kominami, H.; Takada, Y.; Yamagiwa, H.; Kera, Y.; Inoue, M.; Inui, T. *J. Mater. Sci. Lett.* **1996**, *15*, 197.
4. Shi, L.; Li, C.; Chen, A.; Zhu, Y.; Fang, D. *Mater. Chem. Phys.* **2000**, *66*, 51.
5. Sakai, H.; Kawahara, H.; Shimazaki, M.; Abe, M. *Langmuir* **1998**, *14*, 2208.
6. Wu, M.; Long, J.; Huang, A.; Luo, Y.; Feng, S.; Xu, R. *Langmuir* **1999**, *15*, 8822.
7. Chen, J.; Gao, L.; Huang, J.; Yan, D. *J. Mater. Sci.* **1996**, *31*, 3497.
8. Kudo, A.; Miseki, Y. *Chem. Soc. Rev.* **2009**, *38*, 253.
9. Patil, P. P.; Phase, D. M.; Kulkarni, S. A.; Ghaisas, S. V.; Kulkarni, S. K.; Kanetkar, S. M.; Ogale, S. B.; Bhide, V. G. *Phys. Rev. Lett.* **1987**, *58*, 238.
10. Mafuné, F.; Kohno, J.-y.; Takeda, Y.; Kondow, T.; Sawabe, H. *J. Phys. Chem. B* **2000**, *104*, 9111.
11. Hong, S. M.; Lee, S.; Jung, H. J.; Yu, Y.; Shin, J. H.; Kwon, K.-Y.; Choi, M. Y. *Bull. Korean Chem. Soc.* **2013**, *34*, 279.
12. Liu, P.; Cai, W.; Fang, M.; Li, Z.; Zeng, H.; Hu, J.; Luo, X.; Jing, W. *Nanotechnology* **2009**, *20*, 285707.
13. Lee, S.; Ahn, A.; Choi, M. Y. *Phys. Chem. Chem. Phys.* **2012**, *14*, 15677.
14. Iwabuchi, A.; Choo, C.-K.; Tanaka, K. *J. Phys. Chem. B* **2004**, *108*, 10863.
15. Sugimoto, T.; Zhou, X.; Muramatsu, A. *J. Colloid Interface Sci.* **2003**, *259*, 43.